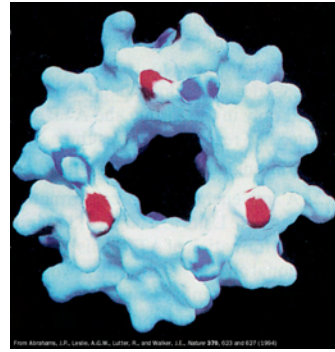
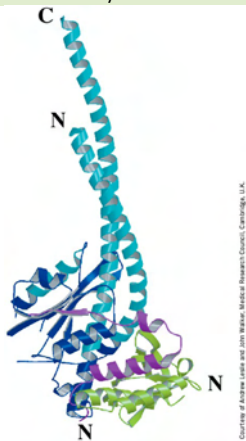


X-Ray structure of F<sub>1</sub>-ATPase from bovine heart mitochondria.

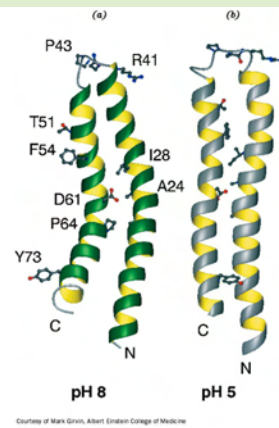


X-Ray structure of F<sub>1</sub>-ATPase from bovine heart mitochondria. The surface of the inner portion of the  $\alpha_3\beta_3$  assembly.

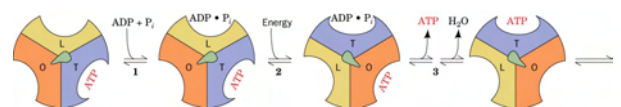
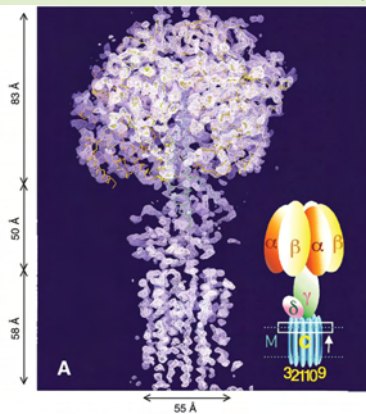
The  $\gamma$ ,  $\delta$ , and  $\epsilon$  subunits in the X-ray structure of bovine F<sub>1</sub>-ATPase.



NMR structures of the c subunit of *E. coli* F<sub>1</sub>F<sub>0</sub>-ATPase.

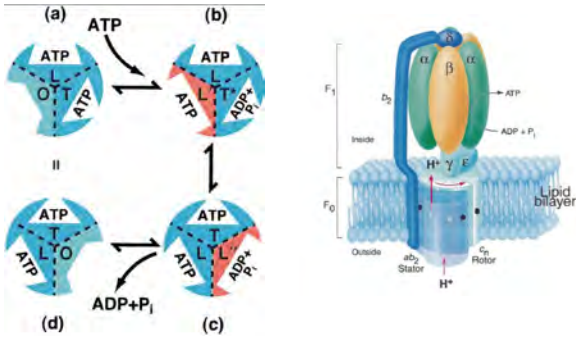


Electron density map of the yeast mitochondrial F<sub>1</sub>-C<sub>10</sub> complex.



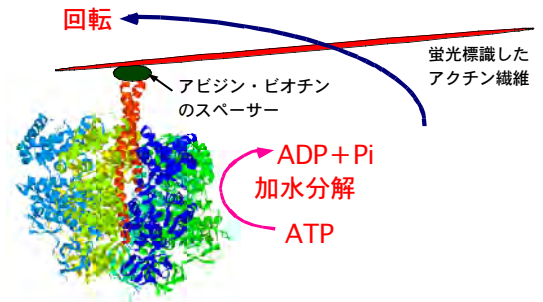
Energy-dependent binding change mechanism for ATP synthesis by proton-translocating ATP synthase.

### ATPaseの構造変化と触媒活性モデル



O(オープン)型: 触媒不活性で基質・生成物に親和性なし  
 L(ルーズ)型: 弱い親和性をもつが、触媒活性なし  
 T(タイト)型: 強い親和性をもち、触媒活性をもつ

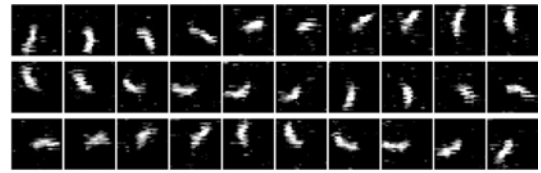
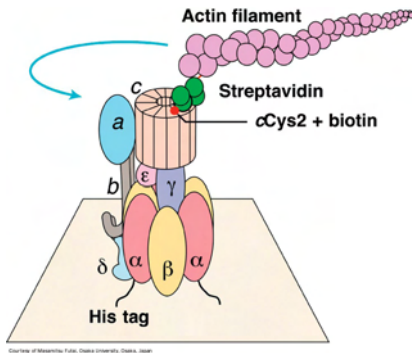
### F型ATPase回転実証の実験系



ATPaseの  $\alpha$   $\beta$   $\gamma$  複合体

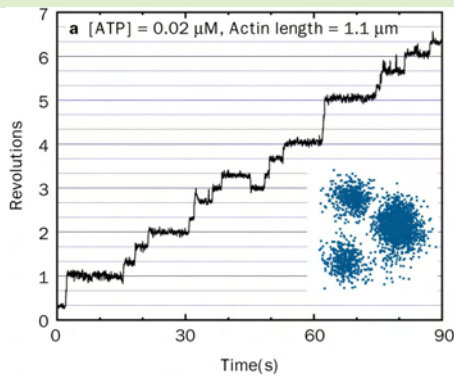
Noji et al. (1997) Nature

### Rotation of the $c$ -ring in *E. coli* $F_1F_0$ -ATPase

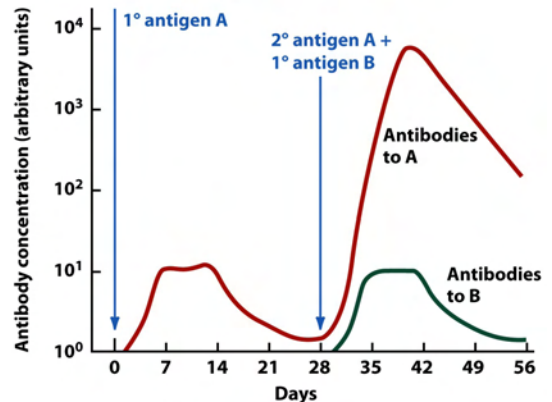


Rotation of the  $c$ -ring in *E. coli*  $F_1F_0$ -ATPase. (b) The rotation of a 3.6- $\mu\text{m}$ -long actin filament in the presence of 5 mM MgATP.

### Stepwise rotation of the $\gamma$ subunit of $F_1$ relative to an immobilized $\alpha_3\beta_3$ unit at low ATP concentration.

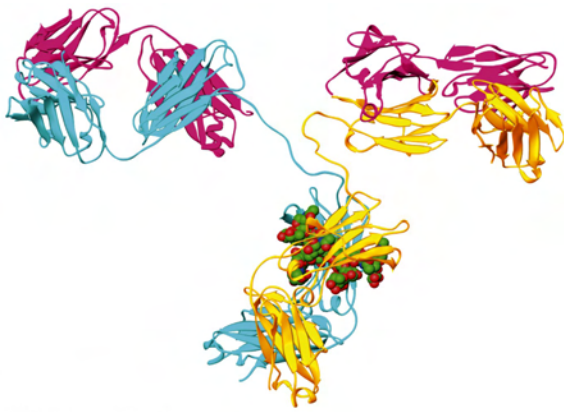


Courtesy of Kazuhiko Arai et al., Keio University, Yokohama, Japan

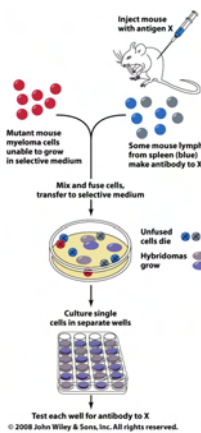
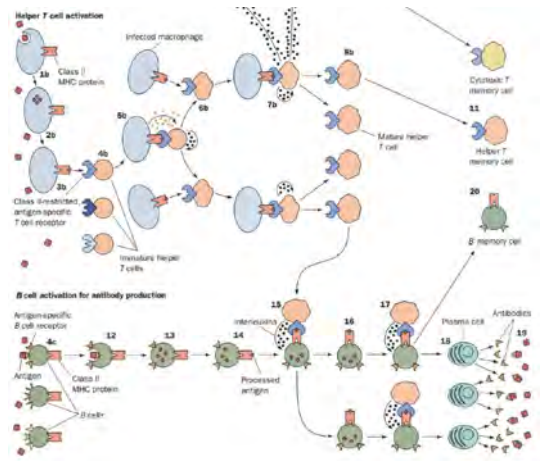


© 2008 John Wiley & Sons, Inc. All rights reserved.

Figure 7-37



© 2008 John Wiley & Sons, Inc. All rights reserved.  
Figure 7-38



Box 7-5

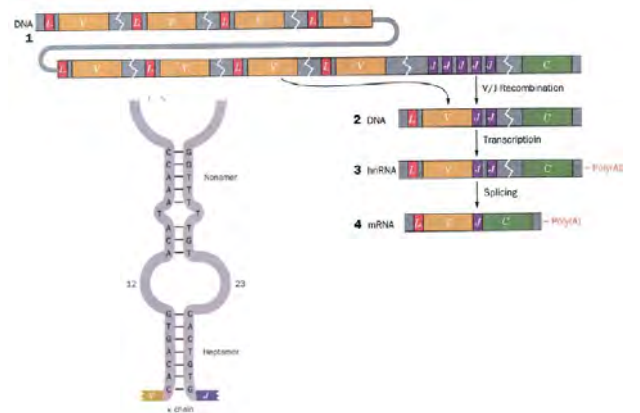


**Table 7-2** Classes of Human Immunoglobulins

Class	Heavy Chain	Light Chain	Subunit Structure	Molecular Mass (kD)
IgA	$\alpha$	$\kappa$ or $\lambda$	$(\alpha_2\kappa_2)_n J^a$ or $(\alpha_2\lambda_2)_n J^a$	360–720
IgD	$\delta$	$\kappa$ or $\lambda$	$\delta_2\kappa_2$ or $\delta_2\lambda_2$	160
IgE	$\epsilon$	$\kappa$ or $\lambda$	$\epsilon_2\kappa_2$ or $\epsilon_2\lambda_2$	190
IgG <sup>b</sup>	$\gamma$	$\kappa$ or $\lambda$	$\gamma_2\kappa_2$ or $\gamma_2\lambda_2$	150
IgM	$\mu$	$\kappa$ or $\lambda$	$(\mu_2\kappa_2)_5 J$ or $(\mu_2\lambda_2)_5 J$	950

<sup>a</sup> $n = 1, 2, \text{ or } 3.$

<sup>b</sup>IgG has four subclasses, IgG1, IgG2, IgG3, and IgG4, which differ in their  $\gamma$  chains

© 2008 John Wiley & Sons, Inc. All rights reserved.

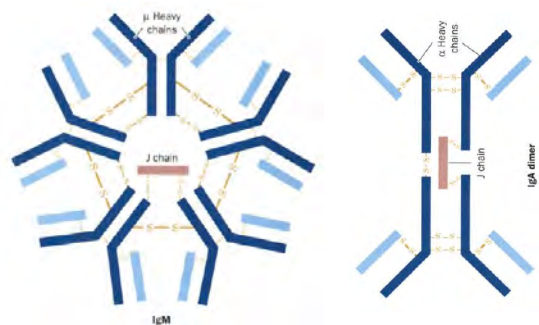
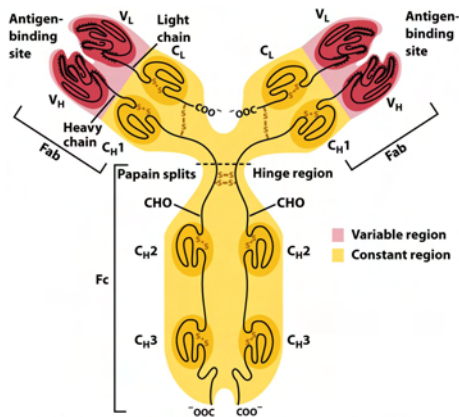
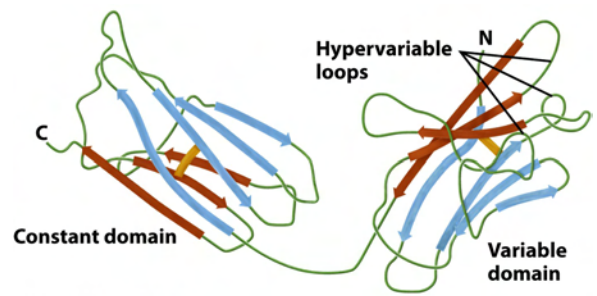


Table 7-2



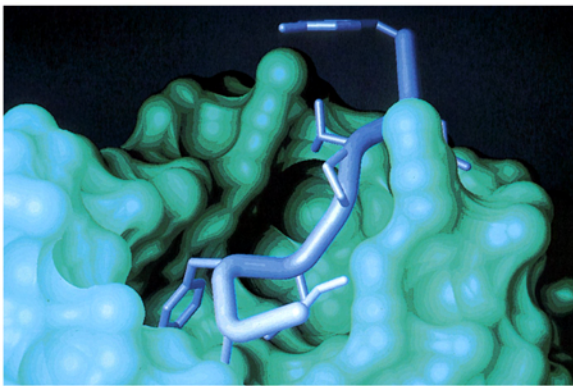
Illustration, Irving Geis. Image from the Irving Geis Collection/Howard Hughes Medical Institute. Rights owned by HHMI. Reproduction by permission only.

Figure 7-39



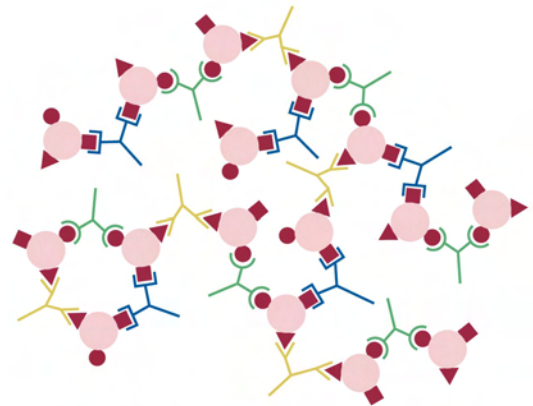
© 2008 John Wiley & Sons, Inc. All rights reserved.

Figure 7-40



Courtesy of Ian Wilson, The Scripps Research Institute, La Jolla, California. PDBid 1HHM.

Figure 7-41



© 2008 John Wiley & Sons, Inc. All rights reserved.

Figure 7-42

Table 7-3 Some Autoimmune Diseases		
Disease	Target Tissue	Major Symptoms
Addison's disease	Adrenal cortex	Low blood glucose, muscle weakness, Na <sup>+</sup> loss, K <sup>+</sup> retention, increased susceptibility to stress
Crohn's disease	Intestinal lining	Intestinal inflammation, chronic diarrhea
Graves' disease	Thyroid gland	Oversecretion of thyroid hormone resulting in increased appetite accompanied by weight loss
Insulin-dependent diabetes mellitus	Pancreatic $\beta$ cells	Loss of ability to make insulin
Multiple sclerosis	Myelin sheath of nerve fibers in brain and spinal cord	Progressive loss of motor control
Myasthenia gravis	Acetylcholine receptors at nerve-muscle synapses	Progressive muscle weakness
Psoriasis	Epidermis	Hyperproliferation of the skin
Rheumatoid arthritis	Connective tissue	Inflammation and degeneration of the joints
Systemic lupus erythematosus	DN A, phospholipids, other tissue components	Rash, joint and muscle pain, anemia, kidney damage, mental dysfunction

© 2008 John Wiley & Sons, Inc. All rights reserved.

Figure 7-3